Study of the Polymer Morphology in Urethane Elastomers by Solid State ^{2}H NMR and Small Angle X-ray Scattering

N. J. Clayden,*,† C. Nijs,‡ and G. Eeckhaut‡

School of Chemical Sciences, University of East Anglia, Norwich, NR4 7TJ, U.K., and ICI, Polyurethanes, Everslaan 45, B-3078 Kortenburg, Belgium

Received June 20, 1997; Revised Manuscript Received July 23, 1998

ABSTRACT: A 4,4′-diphenylmethane diisocyanate (4,4′-MDI)-based poly(ester)−poly(urethane) has been synthesized as selectively ^{2}H labeled at the MDI methylene. The ^{2}H NMR spectrum showed that this elastomer consisted of a rigid and mobile component over a wide temperature range, with the mobile component increasing with temperature. The variation in rigid to mobile transition temperature, T_{RM}, has been analyzed in terms of hard domain imperfections. Empirically, a linear relationship was found between the transition temperature and an imperfection parameter, *i*. SAXS was used to convert the NMR parameters to distances on the basis that the hard domain imperfections were related to the domain size. However, physical mechanisms for obtaining such variations in the domain size do not plausibly explain the variation in T_{RM}. Explanations of the hard domain imperfection consistent with this variation are the misregister of the hard segments and misalignment of hard segments within a hard domain.

1. Introduction

The mechanical properties of polyurethane elastomers are controlled by the microphase structure resulting from incompatible segments of flexible aliphatic polyether (or polyester) alternating with stiff segments originating from isocyanate groups in a block copolymer. Incompatibility of the so-called soft and hard segments leads to a phase separation which is reflected in a rubber-like matrix containing hard microdomains.[1−3] The mechanical strength in this structure can be attributed to hard microdomains cross-linked through hydrogen bonding and dispersion forces, which act as rigid reinforcing particles. As a result, polyurethanes, in general, have a modulus curve which tends to be flat over a wide temperature range, limited at higher temperatures by the melting point of the hard segments. From the point-of-view of the end use applications of polyurethanes it is vital to understand the changes in the mechanical properties with temperature. Of particular interest in this paper are the changes taking place in the hard domains as softening of the polyurethane takes place below 120 °C. Polyurethanes are characterized by a complex morphology[4] dependent upon the precise nature of the hard and soft segments, their composition, and their thermal history. A commerically important class of polyurethanes are those based on 4,4′-diphenylmethane diisocyanate (MDI) chain extended with 1,4-butandiol (BDO). Differential scanning calorimetry of MDI/BDO polyurethanes is consistent with a phase-separated structure with the T_g of the soft matrix elevated by the hard segment dissolved within it,[5] up to a maximum solubility of roughly 30%.[1] Interpretation of the higher temperature endotherms between 50 and 250 °C is less clear-cut; earlier explanations in terms of hydrogen-bonding have now been discounted[6] in favor of models based on the packing order within the hard domains,[7] either multiple crystalline forms based on hard segment lengths or glassy phases. The thermal processes associated with the hard domains are often diffuse and weak at low hard segment contents but give an apparent T_g around 70−90 °C[8] with an additional endotherm around 150 °C attributed to intersegmental mixing. Wide-angle X-ray scattering (WAXS) typically shows an absence of long-range order in the hard domains at the low hard segments fractions[9] typically seen in commercial systems. On the other hand, since crystalline order can be seen in model type polyurethanes[10,11] with a higher hard segment content, it is plausible that the disorder seen in the low hard segment polymers arises from poor alignment of the hard segments within the hard domains, leading to the idea of paracrystalline domains. However, in the absence of WAXS diffraction peaks, little can be inferred about changes in the degree of order of the hard domains with temperature. Infrared spectroscopy has demonstrated that hydrogen bonding is present within the hard domains,[12] and furthermore, as the temperature is increased, the degree of hydrogen-bonding decreases, consistent with the break-up of the hard domains. The presence of order within the hard domains can be observed directly from the frequency of amide carbonyl through the band at 1684 cm^{-1} but can only be inferred from the band-width of the NH stretching frequency at ca. 3300 cm^{-1}.[13] Work on aliphatic isocyanate polyurethanes suggests that the hard domains are mostly disordered with no significant changes in the degree of hydrogen bonding in either ordered or disordered bands up to 110 °C. Qualitative, indirect studies of domain ordering in MDI-based polyurethanes have been done on the basis of polymerization of diacetylene; however, the intensity of the 620 nm absorption was not interpreted in terms of an analytical form for the disorder nor studied as a function of the temperature.[14] Small-angle X-ray scattering can provide the most complete picture of the morphology: the degree of phase mixing, the long period of repeat structures, and the distribution width of domain sizes, as well as whether boundaries are sharp or diffuse.[15−18] Despite this detail, it must be stressed that the interpretations generally use only a simple bulk picture of the morphology, such as a uniform lamellar structure.

† University of East Anglia.
‡ ICI.

10.1021/ma9709009 CCC: $15.00
Published on Web 10/10/1998

Detailed studies have been made on the variation in the SAXS with temperature. Most work has concentrated on identifying the structural changes occurring at high temperatures, above 150 °C, and indeed, at temperatures below this only small changes have been reported, suggesting rather small structural changes.[1,20] It has also been pointed out that at hard segment compositions of less than 40% the hard microdomain structure is discontinuous and therefore the significance of such a measurement is unclear.[21] On the whole, the experimental data is consistent with the model of polyurethane morphology put forward by Koberstein and Stein.[1,15] In this model the thickness of the hard segment domains is controlled by the shortest hard segment chain insoluble in the soft segment phase. Hard segments longer than this must coil or fold over. Hard segments shorter than this are dissolved in the soft segment matrix. Softening of the elastomer with temperature can therefore be understood in terms of a reduced rigidity of the hard domains at the hard−soft domain interphase or a progressive dissolution of the hard segments into the soft phase or both. We can therefore predict at least two types of hard segment dynamics at temperatures well above the T_g of the soft matrix: one with low-amplitude motions, corresponding to hard segments in the hard domain, and the other large-amplitude, high-frequency motions associated with hard segments dispersed in the soft matrix. Evidence for these types of motion can be found in both ^{13}C NMR T_1[22] two-dimensional $^{13}C/^1H$ line shape NMR spectra[23] and in ^2H NMR studies[24−27] of polyurethanes. The ^{13}C relaxation time measurements, made on a *p*-phenylene diisocyanate/BDO hard segment polyurethane, gave upward of 40% of hard segments dispersed in the soft matrix at 30 °C. At the same time, no evidence could be seen for soft segments having a mobility consistent with being in a hard segment rich domain. Similarly, results concerning the absence of soft segments in hard domains of MDI/BDO polyurethanes were obtained from the $^{13}C/^1H$ line shape NMR spectra.[23] No clear picture of hard segment mobility could be deduced, however, because of the weak intensity of the carbon resonances associated with the hard segments.

In one case of ^2H NMR, model polyurethanes were synthesized from hard segments specifically labeled on piperazine rings at different positions in the hard segment.[24,25] A clear motional gradient was seen across the hard segment through a reduction in the quadrupolar splitting in the NMR spectrum with a greater degree of motion evident at a given temperature for the piperazine nearest the soft matrix. This is consistent with the idea of softening at the hard−soft interphase. Equally important, two different types of hard segment were seen at higher temperature in the ^2H NMR spectrum, one corresponding to rigid piperazine rings and the other rings undergoing fast isotropic-like motion. This was seen most clearly when the piperazine were labeled centrally, since the ^2H NMR spectrum showed little evidence for motional averaging within the hard domain. The similarity of the ^2H NMR spectrum with model crystalline systems was taken as evidence for an ordered hard domain, but no attempt was made to quantify this. Significantly, roughly 70% of the ^2H labels in the centrally labeled piperazine were seen to undergo isotropic-like motion 10 K below the melting point, at a temperature where the polymer still exhibited a large dynamics shear modulus.[25] Only 10% of these can be attributed to hard segments dispersed in the soft matrix. In this system there remains the opportunity to explain the presence of the isotropic-like resonance as a tetrahedral jump process within a solid matrix, providing the jump process explores all four tetrahedral sites. Somewhat surprisingly, despite the large increase in the isotropic component, essentially no evidence is presented of intermediate type motions affecting these central piperazine rings before the onset of isotropic-like behavior. Dynamic process have also been seen in the BDO chain extender in an MDI−BDO polyurethane and these have been related to the need for gauche/trans conformational switching to facilitate folding or coiling of hard segments.[26,27] In this instance, the all hard segment MDI/BDO gave a ^2H NMR spectrum consistent with the ^2H labels undergoing two-site tetrahedral jumps in the crystalline hard segments, leading to a broad ∼120 kHz wide NMR line shape up to a temperature of 123 °C.[26] A common feature of both these studies of polyurethane elastomers in which the hard segments have been deuterium labeled was the appearance of a narrow component in the ^2H NMR spectrum, either at room temperature or at higher temperatures.[24,25,27] This narrow component must correspond to hard block segments, carrying a deuterium label, undergoing rapid almost liquid-like isotropic motions with correlation times on the order of 10^{-7}−10^{-8} s. The observation of two types of ^2H NMR line shape indicates that two types of hard block phase must be present. So far, two explanations for this highly mobile component have been presented.[24,25,27] First, deuterated hard segments are dispersed or phase mixed in the soft, rubber-like matrix and, second, the individual hard segments within the crystalline hard block are undergoing rapid pseudo-isotropic motions. However, until now no clear rationale has been presented why the intensity of the highly mobile fraction, as seen by ^2H NMR, should increase with temperature along with softening of the elastomer and at the same time show very little evidence for the presence of intermediate line shapes. The primary objective of the work reported is to offer a general explanation for this temperature variation in terms of a distribution of rigid to mobile transition temperatures, T_{RM}, arising from varying degrees of imperfection or packing defects within the hard domains. In so doing the paper seeks to answer the question whether NMR studies can be used to investigate the nature of the hard domains or whether the observed differences in hard segment dynamics are simply an experimental curiosity. Experimental evidence is based uniquely on an MDI specifically labeled in the central methylene. The principal advantage of this deuteration site is that pseudo-isotropic type motions in the solid state do not appear feasible, any intermediate type motions being based on two-site tetrahedral jumps. Consequently, complications concerning the distinction between pseudo-isotropic motion in the solid state and isotropic motion will not arise. In this paper the rigid to mobile transition temperature is described in terms of the empirical equation 1.

$$T_{RM} = T^*(1 - \alpha i)^{\delta} \qquad (1)$$

where T^* is the transition temperature for the bulk perfect hard domain and i is a measure of the imperfection, with α and δ being fitted parameters. Support for this type of equation can be found in two instances

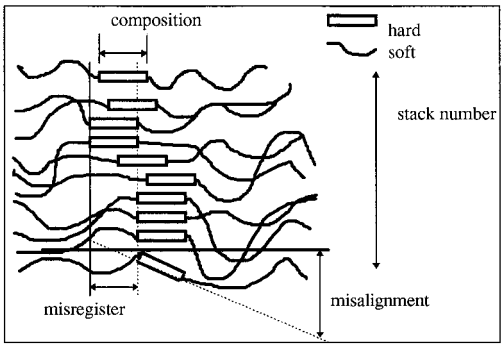

Figure 1. Schematic description of the morphology in a polyurethane elastomer illustrating the hard domain variables.

where the imperfection can be ascribed to the size of the domain with i inversely proportional to the domain size. First, in the case of a crystalline phase, the observed reduction in melting point for a lamellar structure, where l ($i = 1/l$), the thickness of the lamellae, is given by the Thomson−Gibb equation[28] where $\delta = 1$, T^* is the thermodynamic melting point of the perfect crystal, and α depends on the surface energy of the crystal σ_E, the heat of fusion ΔH_f, and the crystal density ρ_c. This would be consistent with the work of Koberstein,[1] where he proposed that the dissolution of hard domains into the soft phase can be considered as a melting process if "noncrystalline" hard segments are treated as "disordered" crystals. Second, for thin films the glass transition temperature has been found to depend on the film thickness for both free-standing[9] and substrate[10]-bound thin films of polystyrene, where the film has a free surface exposed to a vacuum. Theoretical descriptions of this effect have not been deduced, but empirically, the T_g of a film of thickness l ($i = 1/l$) has been found to obey eq 1 with $\delta = 1.8$ in the case of a substrate-bound film and $\delta = -1.0$ for a free-standing film. In both cases, T^* would be the glass transition temperature of bulk hard domain T_g(bulk). An implicit assumption is that, in contrast to the NMR behavior of bulk glassy polymers, once the T_g appropriate for the hard domain is exceeded, the hard segments adopt the dynamics characteristic of the soft matrix in which they are embedded. This assumption is plausible, given the small size of the hard domains as determined by small-angle X-ray scattering. Imperfections in the hard domain can arise not only from size effects related to the stack number and the composition of the hard segments but also from misregister of chains at the start of a hard domain or misalignment within the hard domain, as illustrated in Figure 1. An important consequence of this analysis is that the mobile fraction observed in the ^{2}H NMR spectra will depend on the distribution of the hard domain imperfection, with the more imperfect domains having lower transition temperatures. Superimposed on this general phenomenon will be a real increase in the mobility of the hard segments depending on how far the molecule is from the soft domain interface.[24]

A secondary objective is to examine possible causes of the hard domain disorder shown in Figure 1, such as variations in the domain size, by calculating the expected mobile ^{2}H-labeled fraction. Before this can be carried out, an assumption must be made about the form of the hard domain imperfection distributions. However, despite the wide variety of techniques used to study polyurethanes, there is essentially no data about the nature of the disorder distribution within a hard segment domain. In the absence of knowledge about the true hard domain disorder distribution, a rectangular distribution has been assumed for the purposes of this analysis on the basis of its simplicity. Small-angle X-ray scattering has been used to investigate the morphology independently and in the process provide data necessary to convert the NMR results into absolute distances where the imperfection is interpreted in terms of a domain size distribution.

2. Materials and Methods

2.1. Synthesis of 4,4′-Methylendiphenylene isocyanate-d_2. (I) 4,4′-Diaminodiphenylmethane-d_2. In a four-necked flask fitted with a mechanical stirrer, reflux condenser, thermometer, and dropping funnel, hydrochloric acid with a density of 1.19 kg/L (1.50 mol, 148.0 g) and aniline (3.00 mol, 279.0 g) were mixed and then heated to 50 °C. To this mixture was added deuterioparaformaldehyde (0.18 mol, 16.0 g) dissolved in 160 mL of water dropwise, the temperature of the reaction mixture being kept at 50 °C. The reaction mixture was stirred at 100 °C for 3 h and then cooled to 20 °C. A 5% excess of caustic soda (1.57 mol, 63.0 g sodium hydroxide, in little water) was added. The organic layer was separated from the aqueous layer and washed several times with warm water until neutral and salt free. Excess aniline was removed by steam distillation. The residue was dried in a drying pistol with phosphorus pentoxide to yield 85% of 4,4′-diaminodiphenylmethane-d_2.

(II) 4,4′-methylenediphenylenisocyanate-d_2. A 200 mL portion of dried (molecular sieves) and distilled toluene was introduced in a three-necked flask cooled in an ice bath and fitted with a mechanical stirrer and a dry ice condenser. Over a period of 20 min, phosgene (0.717 mol, 71.0 g) was distilled into the toluene while the temperature was kept at approximately 2 °C. Under vigorous stirring, 4,4′-diaminodiphenylmethane-d_2 (0.125 mol, 25.0 g) dissolved in 215 mL of dry and distilled toluene was pumped into the phosgene/toluene solution through a diptube extending in the phosgene/toluene solution. The whole process of introducing the amine takes about 30 min. The reaction mixture was stirred for another 10 min at 5 °C, after which the ice bath was replaced by a heating mantle. Over a period of 2 h the temperature was gradually increased to 75 °C and kept for another 20 min at this temperature; at this point the reaction mixture was free from solids. After cooling again, the reaction mixture was passed through a thin film evaporator to remove the remaining phosgene, hydrochloric acid, and most of the toluene. The crude 4,4′-methylenediphenylene isocyanate-d_2 was distilled under vacuum. The fraction boiling at 155 °C (0.07 mbar) was collected to yield 95%. The ^{13}C NMR spectrum of 4,4′-methylenediphenylene isocyanate is shown in Figure 2.

Synthesis of the Poly(ester)−Poly(urethane) Elastomer, with Deuterium Labels in the Hard Blocks. The soft block phase of the ^{2}H-labeled polyurethane elastomer is based on a poly(ester)diol, i.e., a bifunctional ethylenetetramethylene adipate of average molecular weight 2000 (Daltocast TA20). This commercial polyester from ICI plc is made in a condensation polymerization of approximately 2 mol adipic acid with 1 mol of ethylene glycol and 1 mol of 1,4-butanediol (1,4-BD). The building blocks of the hard segments of the elastomer are deuterated diphenylmethane 4,4′-diisocyanate (MDI-d_2) and 1,4-butanediol. The molar ratios of the reactants in the elastomer formulation are Daltocast A20/MDI-d_2/l,4-BD = 1.0/3.675/2.5. The procedure for the synthesis of the deuterated elastomer is as follows: TA20 and 1,4-BD are melted out in an oven at 80 °C. MDI-d_2 is distilled under vacuum and kept in an oven at 45 °C. Then a polyol blend is made from TA20 (0.010 mol, 20.00 g) and 1,4-BD (0.025 mol, 2.25 g) both at 80 °C by mixing them together at 3000 rpm for 10 s. Next MDI-d_2 (0.035 mol, 8.82 g) at 45 °C is added to the polyol blend and the mixture is stirred at 3000 rpm for 20 s and degassed under vacuum for 6 min to release the air

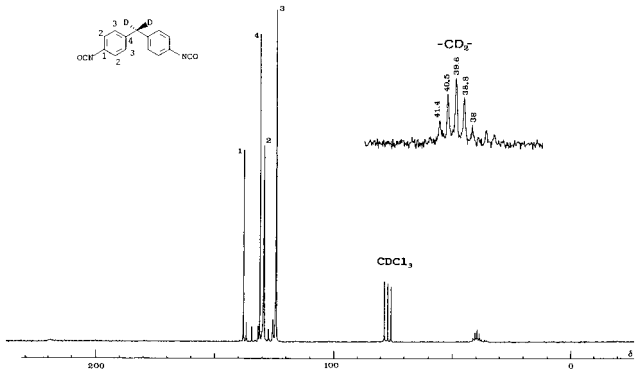

Figure 2. ^{13}C NMR spectrum (^{1}H broadband decoupled) of deuterated 4,4′-methylenediphenylene isocyanate (solvent $CDCl_3$). The inserted detail shows the resonance of the methylene carbon carrying the deuterium labels. The chemical shifts of the multiplet lines are indicated in ppm. The small peaks in the aromatic region are probably due to the presence of the 2,4′-isomer.

bubbles. Then, the reaction mixture is poured into a shallow aluminum mold which has been treated with a mold release agent. The mold is then put in an oven at 80 °C for 16 h. This procedure gave a white, opaque elastomeric film of 0.8 mm thickness. Given this specific stoicheometry for the reactants, the average structure of hard segments in the elastomer contains roughly three MDI and two chain extender units as shown below:

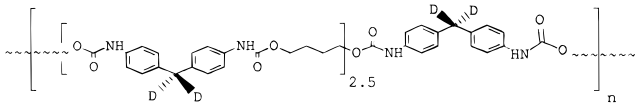

The mass fraction of the hard blocks, calculated from the above formulation, is 0.36 Assuming a hard block density of 1.24, this corresponds to a hard block volume fraction equal to 0.38.

Thermal Analysis. The polyurethane sample was examined by dynamic mechanical thermal analysis (DMTA) and differential scanning calorimetry (DSC). DMTA analysis was carried out on the dynamic mechanical thermal analyzer of Polymer Laboratories. A sample of 1.44 × 7.9 × 2 mm was cut from the elastomeric sheet and analyzed in the single cantilever mode using an oscillation frequency of 1 Hz over a temperature range of −80 to 250 °C at 3 °C/min. The DSC analysis was carried out in a Mettler DSC 30 instrument. The sample (about 15 mg) was cooled from room temperature to −80 °C with a cooling rate of 5 °C/min, then kept 5 min isothermal at −80 °C and then heated to 240 °C at 10 °C/min.

Solid-State ^{2}H NMR. The ^{2}H NMR spectra were acquired on a Bruker MSL200 NMR spectrometer operating at 30.7 MHz. A quadrupole echo pulse sequence $[(\pi/2)_y-\tau_1-(\pi/2)_x-\tau_2]$, combined with phase cycling and an echo delay of 40 μs, was used together with a pulse width of 3.3 μs. This pulse width, equivalent to a $\pi/3$ pulse, was chosen to ensure a faithful excitation of the full bandwidth of the rigid line shape. The rf amplitudes and phase orthogonality were checked prior to data acquisition using a standard multiple pulse tune up procedure on a D_2O sample. Typically 2400 transients were collected at each temperature. A value of τ_2 was chosen to ensure that data acquisition began before the top of the quadruple echo. After data accumulation the free induction decay (FID) was left-shifted by the correct number of points, so that for each spectrum, the part of the FID that was transformed began at the exact top of the echo. Experiments were performed for two different recycle times, corresponding to 3 and 20 s. No differences were seen in the relative intensities of the narrow and broad components over the temperature range studied for these recycle times and therefore it is valid to assume that the NMR spectra are fully relaxed. The echo delay time in the quadrupole echo was

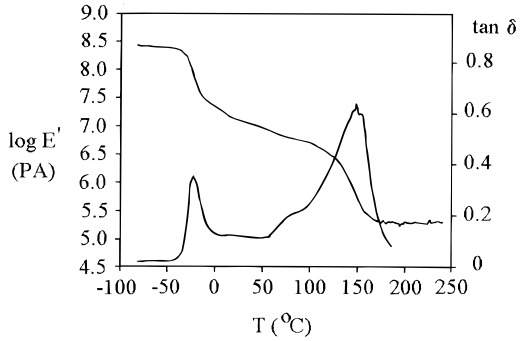

Figure 3. DMTA scan of a poly(ester)−poly(urethane) elastomer with deuterium labels in the MDI hard block (TA20/MDI-d_2/1,4-BD = 1.0/3.675/2.5).

varied at an intermediate temperature of 335 K to see whether there was any preferential reduction in the intensity of the narrow component caused by the quasi-isotropic nature of its motion leading to incomplete refocusing in the quadrupolar echo pulse sequence. As the echo delay was increased, the intensity of the narrow component decreased with respect to the broad one. The effect was not marked, thus when the echo delay was 30 μs the fraction of mobile hard blocks was 0.31, and with a delay of 120 μs the fraction was 0.20. Clearly, if a precise fit to the domain size distribution is required, then the intensities in the quadrupolar echo experiment must be corrected for the different T_{2q}. No correction was made in this case because of the small differences in T_{2q} implied by the NMR spectra when the echo was delayed.

Small-Angle X-ray Scattering. The X-ray data were collected using the small-angle-scattering camera on beam line 2.1 at the SERC Daresbury laboratory, Warrington, U.K. A sample to detector distance of 2.0 m was used, enabling spatial correlations of up 300 Å to be probed over the experimental Q-range of 0.02−0.35 $Å^{-1}$. Parallel plate ionization chambers were placed after and in front of the sample position in order to correct for the decay of the intensity of the incident flux and the X-ray absorption of the elastomer sample. The scattering pattern from an oriented specimen of wet collagen (rat tail tendon) was used to calibrate the sample to detector distance. The SAXS intensities were converted to absolute intensity units of inverse centimeters by using a Lupolene (polyethylene) standard. This standard has been calibrated as a secondary standard from another polyethylene sample ELTEX A1050.[31]

3. Results and Discussion

Thermal Analysis. The results of the DMTA analysis, given in Figure 3, show the presence of two transitions, one centered around −19.5 °C and the other situated around 152 °C. The first transition is the glass transition temperature of the soft block phase, this transition is also present in the DSC scan of Figure 4 but at a lower temperature (around −40 °C). The second transition around 152 °C in the DMTA spectrum, which is much broader than the first one, is related to the melting of the hard block phase. The broad character of this second transition is emphasized further by the DSC results, which show that this second endotherm starts around 130 °C and extends up to 220 °C with a maximum value of dQ/dT around 150 °C. The DMTA results also show that, between these two main transitions, there is a gradual modulus decrease and a clear tan δ jump from 0.1 to 0.3. Between these two transitions, the DSC shows a small endothermic deviation of the baseline which sets in around room temperature and extends as far as the onset of the second transition at 130 °C. The broad endotherm in the DSC is consistent with a distribution in melting points and glass transition temperatures.

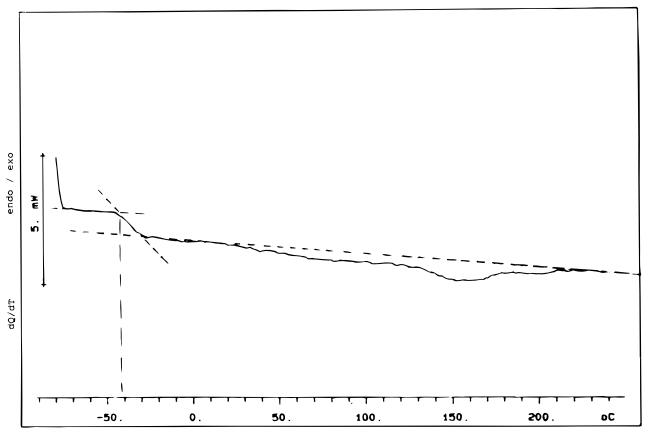

Figure 4. DSC scan of a poly(ester)-poly(urethane) elastomer with deuterium labels in the MDI hard block.(TA20/MDI-d_2/1,4-BD = 1.0/3.675/2.5).

Solid-State NMR. In view of the close relationship expected between the molecular motion of the hard blocks segments and the modulus of the polyurethane, solid-state ^{2}H NMR spectroscopy was employed to characterize the polymer dynamics. The changes taking place in the mobility of the hard block in the intermediate temperature range from 300 to 360 K were of particular importance, since a decrease in modulus was observed over this temperature range. A series of ^{2}H NMR spectra were recorded in the range from 294 to 393 K and are shown in Figure 5. Two components can be identified in the spectra: one, a narrow Lorentzian line shape characteristic of rapid quasi-isotropic motion, and the other, a broad, "Viking" helmet shaped, Pake doublet[32] associated with the low-frequency, low-amplitude motions of the C$-^2$H bonds. In the case of the narrow component, the full width at half-height, $\Delta\nu_{1/2}$ is roughly 8 kHz at 300 K, decreasing to a plateau value of about 5 kHz above 340 K, suggesting only a small change in the frequency of the fast motions with temperature. For the broad component, the splitting is 120 kHz at 300 K, close to that expected for a rigid C$-^2$H group. Furthermore, even at 393 K, the broad component still shows a splitting of 120 kHz with no evidence for rounding of the horns of the pattern as would be expected if intermediate frequency motions are present. The solid-state ^{2}H NMR spectrum therefore originates apparently from a population of highly mobile and rigid hard blocks. On the basis of this observation, a model is proposed involving a rigid to mobile transition of hard blocks to describe the temperature dependence of the solid-state NMR spectrum and hence the thermally induced motions of the C$-^2$H bonds. The line shape originating from the rigid C$-^2$H bonds was calculated from the expression given by Abragam[33] eq 2

$$\nu = \nu_o \pm \frac{3e^2qQ}{8h}(3\cos^2\theta - 1.0 + \eta\sin^2\theta\cos 2\phi) \quad (2)$$

where ν_o is the Zeeman frequency and e^2qQ/h the quadrupolar coupling constant (QCC); the asymmetry parameter, η, describes the deviation of the electric field gradient tensor (EFG) from axial symmetry in the principal axis system (PAS), and θ and ϕ are the polar and azimuthal angle locating the magnetic field vector β_o in the PAS of the EFG.

In the case of deuterons and in the absence of motion, e^2qQ/h equals approximately 165 kHz with only minor variations, and the asymmetry parameter is very close to zero because the EFG is axially symmetric around the C$-^2$H bond direction. Thus for each orientation of the C$-^2$H bond in the rigid sample, a splitting is observed according to eq 2 where the + and − signs correspond to the two allowed NMR transitions. In an isotropic sample where all the possible orientations of the C$-^2$H bonds are equally probable the resulting "powder" line shape is the Pake[32,33,34] spectrum of the $I = 1$ spin system.

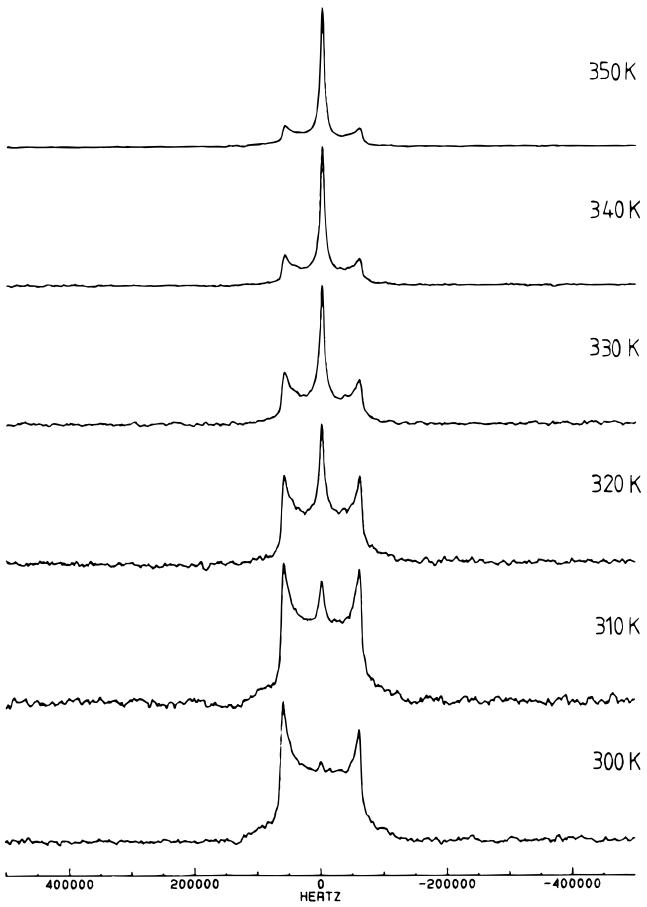

Figure 5. Experimental solid state 30.7 MHz ^{2}H NMR spectra of the poly(ester)−poly(urethane) elastomer as a function of temperature. On the right-hand side of the spectra the nominal temperatures indicated by the temperature control unit are given.

The NMR line shape originating from the highly mobile C$-^2$H fraction can be understood in terms of a fast pseudo-isotropic motional averaging of the quadrupolar interaction. In the limit this will make the Pake doublet collapse into a narrow Lorentzian component. The experimental lines were calculated using a linear combination of two basic band shapes, the Pake pattern for the rigid C$-^2$H component and the Lorentzian for the mobile one. Fitting was carried out using a SIMPLEX routine comparing the observed and calculated ^{2}H NMR spectra. Five variables were used; the quadrupole coupling constant and line widths for both the mobile and rigid components together with the fraction of the mobile component. In the simulation of the experimental NMR spectra, corrections have been made for the finite pulse length and pulse power falloff as a function of frequency. However, the effect of the molecular motions during the radio frequency pulses has not been taken into account.[35,36] To account for the dipolar interactions between neighboring ^{2}H and ^{1}H

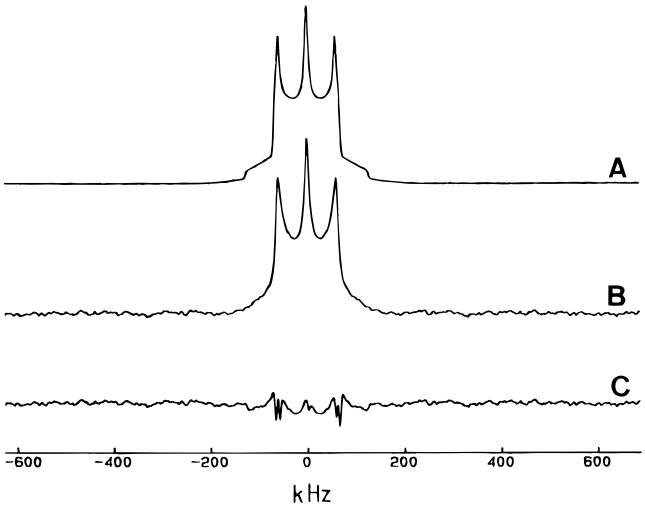

Figure 6. Best fit calculated ^{2}H NMR spectrum from a SIMPLEX fit to the experimental NMR data at a calibrated temperature of 325 K. Fitted mobile fraction $\phi_M = 0.08$.

magnetic dipoles, the Pake pattern was broadened by convolution with a Gaussian function.[37−41] After the Pake pattern is calculated, a Lorentzian component originating from the mobile fraction of C−^{2}H moieties is added such that the new composite line shape approximates as closely as possible the experimental line shape. A typical example of the experimental and simulated solid-state NMR line shapes is shown in Figure 6 as well as the fraction of mobile and rigid C−^{2}H moieties that were obtained in the fitting procedure. Rigid lattice line shapes for the hard blocks are not too surprising given the constraints imposed on large amplitude motions for the central methylene in the MDI unit by the packing of the individual hard segments into the hard blocks. Support for this view is provided by the ^{2}H NMR spectrum of 4,4′-diphenylmethane bis-(butylbenzylphenylene-4-carbamato)carbamate-d_2. This compound, which is a chemically very similar to the hard segments of the 1,4-butanediol chain-extended hard segments, gave a rigid lattice line shape even at 371 K, which is about 94 K below its melting point.

The appearance of the narrow line component with a width of less than 10 kHz at higher temperatures in the case of the elastomer indicates the presence of C−^{2}H bonds undergoing rapid molecular motions (>108 kHz) exploring all orientations or C−^{2}H bonds undergoing tetrahedral jumps or a combination of both. Previous studies have assumed that the motionally averaged peak originates from individual hard segments dispersed in the soft block phase. If that were to be the case for the elastomer under investigation, one would expect that above a certain temperature, corresponding to the temperature above which all the dispersed hard segments are highly mobile, that is 50−60 K above the glass transition temperature of the soft segments,[25] a plateau value for the mobile fraction would be obtained, until a high enough temperature is reached whereupon the bulk of the hard blocks starts to melt. This behavior is not consistent with the experimental results presented, which indicate a gradual and continuous increase of the mobile fraction as the temperature increases. Indeed, given that the glass transition temperature of the soft segments is around 233 K, any hard block dispersed in the soft block can be expected to be pseudo-isotropically mobile[25] at 283−293 K. Yet no mobile hard block is seen at this temperaure.

The model proposed here is that the changes in the ^{2}H NMR spectrum are probably best understood in terms of a broad distribution of rigid to mobile transition temperatures from either a glassy or crystalline hard block phase, caused by their differing degrees of imperfection. Examination of the DSC trace in Figure 4 shows indeed a broad endothermic transition smeared out over a wide temperature range. Previous workers have attributed these transitions to the effect of hard segment length segregation, suggesting hard domains of differing size or packing. Thermal decomposition is unlikely to be relevant to these NMR studies, since it occurs at temperatures in excess of 160 °C. The explanation of the variation in mobility of the hard segments in terms of a rigid to mobile transition process similar to melting could account for the absence of intermediate dynamic freedom or partial motional averaging. If these effects were present they would clearly show up in a more "tapered" appearance[25] of the solid-state NMR lines at the intermediate temperatures, which is clearly not the case in the experimental spectra of Figure 5. A second indicator of the absence of partial motional averaging is the constant width of the Pake doublet at half-height (128 ± 2 kHz) and the constant separation of the quadrupolar splitting peaks (121 ± 2 kHz). When partial motional averaging occurs, it clearly shows up as a gradual decrease in the width at half-height of the Pake doublet and a decrease in the splitting between the quadrupolar peaks,[25] two phenomena which are clearly absent in the presented spectra. The absence of this partial motional averaging suggests dynamics similar to a melting process in which at a particular temperature a certain fraction of the hard blocks suddenly and completely disintegrates into the individual hard segments of which it was comprised. In this process the hard segments are transferred from a highly rigid state to a highly mobile state without intermediate motional regimes. The nature of this change in mobility would seem to argue against the rigid to mobile transition being a glass-transition since such transitions in the bulk usually show gradual and continuous changes in NMR parameters only giving rise to spectral collapse at temperatures well above T_g. However, it is plausible that because of their small size the hard domains, once they pass through their glass-transition temperature, rapidly adopt the dynamics characteristic of the surrounding soft segment matrix.

A general quantitative description of the variation in transition temperatures is given by eq 1. In terms of this equation, at any given temperature, the fraction of hard block segments that has undergone the rigid to mobile transition will simply be the fraction of hard blocks domains with a domain imperfection greater than a defined value $F(i>i_T)$. Thus at low temperatures the mobile hard segment fraction corresponds to segments originally located in very imperfect domains, and as the temperature is increased, more ordered domains undergo a rigid to mobile transition until finally all the hard blocks have "melted".

Further analysis of the NMR data requires that assumptions are made about the nature of the distribution representing the hard block imperfections. As a first approximation, a rectangular distribution was chosen, principally because it has the merit of giving a simple relationship between the temperature T and the mobile hard block fraction $F(i>i_T)$ as shown in eq 3

$$F(i>i_T) = \kappa[(1 - T/T^*)^{1/\delta} - (1 - T_{min}/T^*)^{1/\delta}] \quad (3)$$

A SIMPLEX analysis of $F(i>i_T)$ was carried out allowing κ, T_{min}, T^*, and δ to be varied. The variables κ and T^* are in fact interdependent, and only the ratio T^*/κ is a constant, hence, the quality of the fit cannot be assessed on the value of T^* determined in the fit. The experimental data were found to be rather insensitive to the precise functional form and a range of values was obtained for δ, T_{min}, and T^*/κ depending on the initial values chosen for the SIMPLEX vertexes. For wide variations in the initial parameters, however, an acceptable fit corresponding to a χ^2 of less than 9.0 could be obtained with T_{min} in the range 311.0 ± 2 K, $\delta = 1.0 \pm 0.1$ and $T^*/\kappa = 128.0 \pm 2$ K, indicating a linear relationship between the disorder parameter and the transition temperature. Excellent agreement is seen between the first onset of a mobile fraction in the ^{2}H NMR spectrum and T_{min}. A comparison of the observed and calculated mobile fraction for the best fit is shown in Figure 7. In view of the insensitive nature of the fitting procedure, detailed analysis was restricted to the rectangular distribution. However, preliminary analysis based on a truncated Gaussian distribution indicates that the general conclusions in terms of a relationship between the disorder and the transition temperature are not specific to the chosen distribution. One interpretation of the disorder parameter i is in terms of a domain size distribution. This requires the input of a scaling factor from SAXS to convert the above distribution parameters to a distance one.

Small-Angle X-ray Scattering. The small-angle X-ray scattering one-dimensional correlation function and its Fourier transform are shown in Figures 8 and 9, respectively. Examination of the one-dimensional correlation function indicates a maximum located at 110 Å. Furthermore, the broad SAXS peak implies a wide distribution in the size of the hard and soft block domains. On the basis of the maximum at 110 Å in the one-dimensional correlation function together with an estimated hard block volume fraction of 0.3, from the chemical formulation of the elastomer, and assuming a Gaussian distribution for the hard blocks present, an average thickness of the hard blocks of around 33 Å can be derived. This value is in reasonable agreement with the single-crystal X-ray data of Born et al.[43,44] for 1,4-butanediol/4,4-MDI model compounds. From Born's[43,44] data is it possible to calculate that an average hard block segment of three MDI and two butanediols is about 44 Å. Taking these values as the upper and lower limits for the average thickness of the hard blocks, the width of the distribution implied by the NMR data can be estimated. An important feature of this analysis is the relative independence of the distribution width on the precise functional relationship used to describe the variation of transition temperature with domain size. For example, with the rectangular distribution the best fit linear model gave $l_{min} = 26.8$ Å, $l_{max} = 39.2$ Å. To relate these values to the morphology of the polyurethane the various ways in which the hard domain size can vary must be considered. One model of the morphology presented earlier is that of hard domains formed by stacks of MDI segments embedded in a soft matrix, shown in Figure 1, where the domain is of variable stack number. In this picture the smallest dimension can be either the width of the hard segment or the stack number. In the former case the width will

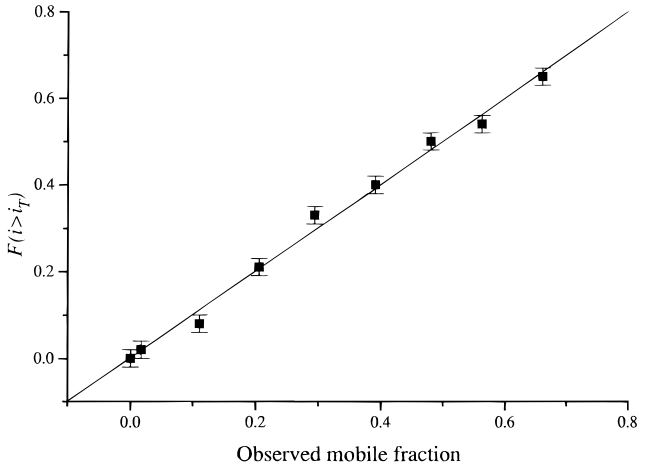

Figure 7. Plot of the observed mobile fraction, $F(i>i_T)$, against the calculated mobile for a rectangular distribution of the hard block disorder parameter for best fit solution found in the SIMPLEX fitting based on eq 3. The line represents a linear regression of the observed and calculated mobile fraction with a correlation coefficient of 0.996.

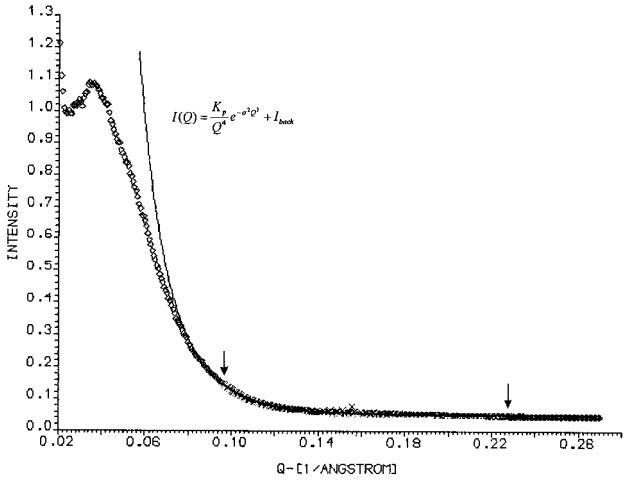

Figure 8. Small-angle X-ray spectrum (SAXS) of the poly(ester)−poly(urethane) elastomer. Intensity is in absolute units (cm^{-1}) and the momentum transfer Q in $Å^{-1}$.

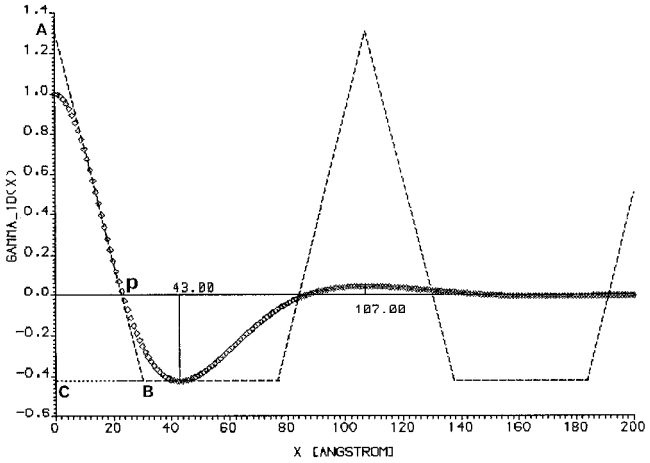

Figure 9. One-dimensional correlation function for the poly(ester)−poly(urethane) elastomer.

be determined by the register of the hard segments and their average composition, that is, the number of MDI fragments and chain extender joined together. The reason for emphasizing the smallest dimension is because the distances deduced from the transition

temperature model, where the disorder is interpreted as a dimension, represent the smallest physical dimension of the domain. Other dimensions can, but need not, be orders of magnitude different. On the basis of the morphology in Figure 1, there are three possible explanations of the distribution seen in the smallest hard domain dimension: (1) the hard block composition, (2) the number of hard segments stacked together, and (3) misregister in the start of the hard domain segments. It must be noted that none of these taken on their own present a convincing case for a domain size variation consistent with an increase in T_g. In particular, only the third explanation can give a continuous distribution in a domain dimension, the first two of necessity will give a discrete distribution based on either the length of the MDI unit or the separation between the MDI units, which lead to incremental dimensions on the order of 10 and 4 Å, respectively. Thus, changes in the hard block composition can only account for the narrow distribution if we consider a complete stack and determine an average composition across the stack. However, using this model there is no compelling argument to explain why a domain of irregular thickness has thermal properties approximating those of the average domain thickness. Misregister of the start of the hard domains will allow somewhat larger domains, but it cannot generate a length less than that of hard segments in perfect register. Moreover, it is arguable whether the larger domain will have an increased T_g; indeed, as the misregister increases, the likelihood is that this will act as a fault within a stack and lead to a lower T_g. Paradoxically then, an increase in one dimension of the domain would bring about a lower T_g. Consequently, misregister cannot provide a physical model for the variation in the T_g with domain size. Equally, variations in the stack number do not seem plausible as an explanation because the resulting distribution is discrete and would correspond to only a few stack numbers, roughly 10 ± 2, assuming 4 Å separation between the MDI units. Consequently, although the ^{2}H NMR data is consistent with the explanation as a domain size dependent rigid to mobile transition temperature, the actual descriptions of how the smallest domain dimension can vary do not provide an adequate physical picture for a change in the transition temperature. Thus, we must turn to other features of the hard domain. A qualitative explanation for a variation in T_{RM} can be found in the idea of the disorder within the hard domain where imperfections would arise from misregister of the start of the hard segments and misalignment of the hard segment chains within a domain. Increasing misregister and misalignment will lead to a more disordered, imperfect hard domain and thus a lower rigid to mobile transition temperature. Empirically, a relationship of the form shown in eq 1 could be consistent with misregister, providing the parameter i represents the standard deviation of the misregister distribution; were i to represent simply the average misregister, then the situation is the same as for the average composition, where questions remain about how this can translate into a transition temperature. Using the variance it is more straightforward to envisage how a very "rough" surface has a different T_{RM} from a smooth one. Misalignment can be similarly treated only in this case; i would represent the spread of the hard segment chain axis from the average direction. Thus, ideas of hard block perfection can be accommodated within a functional description previously shown to be consistent with the NMR data. Of course, it must be borne in mind that these are purely empirical and suffer from the weakness that the observed temperature dependence cannot be used to derive the distance misregister or angular misalignment without some external normalization. However, as an example inserting an arbitrary average misregister standard deviation of 5 Å into eq 1 and assuming a rectangular distribution leads to a minimum misregister of 4 Å to a maximum of 6 Å. The sensible range derived indicates that the use of this equation does not lead to physically unrealistic values. Consequently, although the actual extent of imperfections cannot be deduced from the parameters derived from the analysis of the NMR data, these parameters do provide a way of characterizing the morphology in the poly(ester)−poly(urethane) and thus allow comparison of different formulations and processing conditions.

4. Conclusions

A polyurethane elastomer based on a polyester diol as the soft block and 1,4-butanediol as chain extender which has been selectively deuterated in the hard block has been studied by ^{2}H NMR spectroscopy and SAXS. The ^{2}H NMR spectra can be described in terms of a rigid and highly mobile component. Little evidence was seen for a rapid quasi-isotropic motion in the crystalline hard blocks which would be necessary if the temperature dependence of the hard segment mobility is interpreted as an increase of dynamic freedom within the solid hard block domains. As the temperature is increased, so too does the fraction of the mobile hard block segments. This can be interpreted in terms of a rigid to mobile transition similar to a melting process of the hard block domains into the soft block matrix, consistent with Koberstein's picture of the microphase structure. The distribution of the rigid to mobile temperatures for the hard block domains was related to disorder parameter assuming an empirical relationship. Evidence supporting the view that a variety of rigid to mobile transition temperatures are present is provided by the DSC trace, where a broad endotherm is seen corresponding to the melting of hard block domains. The absence of intermediate mobility regimes for the C−^{2}H bonds in the hard segments further substantiates the view that a process with dynamics similar to melting is present which sets in just above room temperature for the very disordered domains, rather than motion within a rigid hard block phase. The temperature dependence of the ^{2}H NMR spectrum was consistent with a linear decrease in the rigid to mobile transition temperature with a disorder parameter; however, interpretations of this parameter in terms of a variation in a hard domain size do not provide an adequate explanation for the change in T_{RM}. A qualitative explanation can be found in the intrinsic disorder within a hard domain. Misregister and misalignment within the hard domain lead to greater disorder and thus a lower T_{RM}. Empirical quantitative relationships between these factors and the T_{RM} were deduced from the variation in the mobile fraction with temperature. At present, it is not possible to convert the NMR distribution parameters into distance or angular factors related directly to the disorder descriptors. The NMR distribution parameters do allow a comparison between elastomers with different hard segment and soft segment composition.

Acknowledgment. We thank ICI, Polyurethanes for permission to publish this work.

References and Notes

(1) Koberstein, J. T.; Russell, T. P. *Macromolecules* **1986**, *19*, 714.
(2) Estes, G. M.; Huh, D. S.; Cooper, S. L. In *Block Polymers;* Aggerwall, S. L., Ed.; Plenum Press: New York, 1970.
(3) Seymour, R. W.; Estes, G. M.; Cooper, S. L. *Macromolecules* **1970**, *3*, 579.
(4) Yoon, S. C.; Ratner, B. D. *Macromolecules* **1988**, *21*, 2392.
(5) Wood, L. A. *J. Polym. Sci.* **1958**, *28*, 319.
(6) Samuels, S. L.; Wilkes, G. L. *J. Polym. Sci. Polym Symp.* **1973**, *43*, 149.
(7) Koberstein, J. T.; Galambos, A. F. *Macromolecules* **1992**, *25*, 5618.
(8) MacKnight, W. J.; Yang, M.; Kajiyama, T. *Polym. Prepr. (Am. Chem. Soc. Div. Polym.* Chem) **1968**, *9* (1), 860.
(9) Martin, D. J.; Meijs, G. F. Renwick, G. M.; Renwick, G. M.; Gunatillake, P. A.; McCarthy, S. J. *J. Appl. Polym. Sci.* **1996**, *60*, 557.
(10) Vallance, M. A.; Castles, J. L.; Cooper, S. L. *Polymer* **1984**, *25*, 1734.
(11) Hwang, K. K. S.; Wu, G.; Lin, S. B.; Cooper, S. L. *J. Polym. Sci. Polym. Chem. Ed.* **1984**, *22*, 1677.
(12) Seymour, R. W.; Cooper, S. L. *Macromolecules* **1973**, *16*, 48.
(13) Coleman, M. M.; Lee, K. H.; Skrovanek, D. J.; Painter, P. C. *Macromolecules* **1986**, *19*, 2149.
(14) Nitzsche, S. A.; Hsu, S. L.; Hammond, P. T.; Rubner, M. F. *Macromolecules* **1992**, *25*, 2391.
(15) Koberstein, J. T.; Stein, R. S. *J. Polym. Sci. Polym. Phys. Ed.* **1983**, *21*, 1439.
(16) Ryan, A. J.; Macosko, C. W.; Bras, W. *Macromolecules* **1992**, *25*, 6277.
(17) Martin, D. J.; Meijs, G. F.; Gunatillake, P. A.; McCarthy, S. J.; Renwick, G. M. *J. Appl. Polym. Sci.* **1997**, *64*, 803.
(18) Leung, L. M.; Koberstein, J. T. *J. Polym. Sci. Polym. Phys. Ed.* **1985**, *23*, 1883.
(19) Chang. S. L.; Yu, T. L.; Huang, C. C.; Chen, W. C.; Linliu, K.; Lin, T. L. *Polymer* **1998**, *39*, 3479.
(20) Li, Y.; Gao, T.; Liu, J.; Linliu, K.; Desper, C. R.; Chu, B. *Macromolecules* **1992**, *25*, 7365.
(21) Koberstein, J. T.; Galambos, A. F.; Leung, L. M. *Macromolecules* **1992**, *25*, 6195.
(22) Ishida, M.; Yoshinaga, K.; Horii, F. *Macromolecules* **1996**, *29*, 8824.
(23) Tao, H.; Rice, D.; MacKnight, W. J.; Hsu, S. L. *Macromolecules* **1995**, *28*, 4036.
(24) Meltzer, A. D.; Spiess, H. W.; Eisenbach, C. D.; Hayen, H. *Macromolecules* **1992**, *25*, 993.
(25) Kornfield, J. A.; Spiess, H. W.; Nefzger, H.; Hayen, H.; Eisenbach, C. D. *Macromolecules* **1991**, *24*, 4787.
(26) Kintanar, A.; Jelinski, L. W.; Gancarz, I.; Koberstein, J. T. *Macromolecules* **1986**, *19*, 1876.
(27) Dumais, J. T.; Jelinski, L. W.; Leung, L. L.; Gancarz, I.; Galambos, A.; Koberstein, J. T. *Macromolecules* **1985**, *18*, 116.
(28) Wunderlich, B. *Chem. Phys.* **1958**, *29*, 139.
(29) Forrest, J. A.; Dalnoki-Veress, K.; Stevens, J. R.; Dutcher, J. R. *Phys. Rev. Lett.* **1996**, *77*, 2002.
(30) Keddie, J. L.; Jones, R. A. L.; Cory, R. A. *Europhys. Lett.* **1994**, *27*, 59.
(31) Russell, T. P.; Lin, J. S.; Spooner, S.; Wignall. G. D. *Appl. Cryst.* **1988**, *21*, 629.
(32) Pake, G. E. *J. Chem. Phys.* **1948**, *61*, 327.
(33) Abragam, A. *Principles of Nuclear Magnetism*; Oxford University Press: Oxford, 1961.
(34) Spiess, H. W. *Colloid Polym. Sci.* **1983**, *261*, 193.
(35) Bloom, M.; Davies, J. H.; Valic, M. I. *Can. J. Phys.* **1980**, *58*, 1510.
(36) Barbara, T. M.; Greenfield, M. S.; Vold, R. L.; Vold, R. R. *J. Magn. Reson.* **1986**, *69*, 311.
(37) Hentschel, D.; Sillescu, H.; Spiess, H. W. *Makromol. Chem.* **1979**, *180*, 241.
(38) Pschorn, O.; Spiess, H. W. *J. Magn. Reson.* **1980**, *39*, 217.
(39) Hirshinger, J.; Miura, H.; Gardner, K. H.; English, A. D. *Macromolecules* **1990**, *23*, 2153.
(40) Miura, H.; Hirshinger, J.; English, A. D. *Macromolecules* **1990**, *23*, 2169.
(41) Komoroski, R. A.; Lehr, M. H.; Goldstein, J. H.; Long, R. C. *Macromolecules* **1992**, *25*, 3381.
(42) Henrichs, P. M.; Hewitt, J. M.; Linder, J. *J. Magn. Reson.* **1984**, *60*, 280.
(43) Quay, J. R.; Blackwell, J.; Lee, C. D.; Hespe, H.; Born, L. J. *Macromol. Sci.-Phys.* **1985**, *B24*, 61.
(44) Born, L.; Crone, J.; Hespe, H.; Muller, E. H.; Wolf, K. H. *J. Pol. Sci.-Polym. Phys. Ed.* **1984**, *22*, 163.

MA9709009